

AD-A131 667

BOUNDARY-INTEGRAL SIMULATIONS OF RAYLEIGH-TAYLOR
INSTABILITY IN IDEAL MAGNETOHYDRODYNAMICS(U) CAMBRIDGE
HYDRODYNAMICS INC MA G R BAKER ET AL. AUG 83

1/1

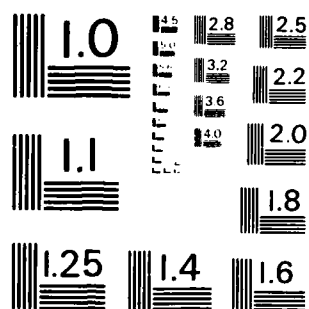
UNCLASSIFIED

AFWL-TR-83-12 F29601-82-C-0036

F/G 20/9

NL

END
DATE
FILMED
#0 - 10-1
DTIC



MICROCOPY RESOLUTION TEST CHART
NATIONAL BUREAU OF STANDARDS - 1963 - A

ADA 131667



**BOUNDARY-INTEGRAL SIMULATIONS
OF RAYLEIGH-TAYLOR INSTABILITY
IN IDEAL MAGNETOHYDRODYNAMICS**

Gregory R. Baker
Robert L. McCrory
Steven A. Orszag

Cambridge Hydrodynamics, Inc.
54 Baskin Road
Lexington, MA 02173

August 1983

Final Report

Approved for public release; distribution unlimited.

AIR FORCE WEAPONS LABORATORY
Air Force Systems Command
Kirtland Air Force Base, NM 87117

DTIC
ELECTE
AUG 23 1983
S A D

DTIC FILE COPY

83 08 22 06 9

This final report was prepared by the Cambridge Hydrodynamics, Inc., Lexington, Massachusetts, under Contract F29601-82-C-0036, Job Order 88091701 with the Air Force Weapons Laboratory, Kirtland Air Force Base, New Mexico. Major Brian J. Kohn (NTYP) was the Laboratory Project Officer-in-Charge.

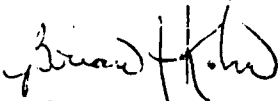
When Government drawings, specifications, or other data are used for any purpose other than in connection with a definitely Government-related procurement, the United States Government incurs no responsibility or any obligation whatsoever. The fact that the Government may have formulated or in any way supplied the said drawings, specifications, or other data, is not to be regarded by implication, or otherwise in any manner construed, as licensing the holder, or any other person or corporation; or conveying any rights or permission to manufacture, use, or sell any patented invention that may in any way be related thereto.

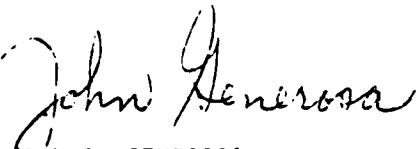
This report has been authored by a contractor of the United States Government. Accordingly, the United States Government retains a nonexclusive, royalty-free license to publish or reproduce the material contained herein, or allow others to do so, for the United States Government purposes.

If your address has changed, if you wish to be removed from our mailing list, or if your organization no longer employs the addressee, please notify AFWL/NTYP, Kirtland AFB, NM 87117 to help us maintain a current mailing list.

This report has been reviewed by the Public Affairs Office and is releasable to the National Technical Information Service (NTIS). At NTIS, it will be available to the general public, including foreign nations.

This technical report has been reviewed and is approved for publication.


BRIAN J. KOHN
Major, USAF
Project Officer


JOHN I. GENEROSA
Lt Colonel, USAF
Chief, Simulators & Advanced
Weapons Concepts Branch

FOR THE COMMANDER

ALAN R. COLE
Colonel, USAF
Chief, Advanced Technology Division

DO NOT RETURN COPIES OF THIS REPORT UNLESS CONTRACTUAL OBLIGATIONS OR NOTICE ON A SPECIFIC DOCUMENT REQUIRES THAT IT BE RETURNED.

UNCLASSIFIED

SECURITY CLASSIFICATION OF THIS PAGE (When Data Entered)

REPORT DOCUMENTATION PAGE		READ INSTRUCTIONS BEFORE COMPLETING FORM
1. REPORT NUMBER AFWL-TR-83-12	2. GOVT ACCESSION NO. AD-A131667	3. RECIPIENT'S CATALOG NUMBER
4. TITLE (and Subtitle) BOUNDARY-INTEGRAL SIMULATIONS OF RAYLEIGH-TAYLOR INSTABILITY IN IDEAL MAGNETOHYDRODYNAMICS		5. TYPE OF REPORT & PERIOD COVERED Final Report
		6. PERFORMING ORG. REPORT NUMBER
7. AUTHOR(s) Gregory R. Baker Robert L. McCrory Steven A. Orszag		8. CONTRACT OR GRANT NUMBER(s) F29601-82-C-0036
9. PERFORMING ORGANIZATION NAME AND ADDRESS Cambridge Hydrodynamics, Inc. 54 Baskin Road Lexington, MA 02173		10. PROGRAM ELEMENT, PROJECT, TASK AREA & WORK UNIT NUMBERS 62601F/88091701
11. CONTROLLING OFFICE NAME AND ADDRESS Air Force Weapons Laboratory (NTYP) Kirtland Air Force Base, NM 87117		12. REPORT DATE August 1983
		13. NUMBER OF PAGES 34
14. MONITORING AGENCY NAME & ADDRESS (if different from Controlling Office)		15. SECURITY CLASS. (of this report) Unclassified
		15a. DECLASSIFICATION DOWNGRADING SCHEDULE
16. DISTRIBUTION STATEMENT (of this Report) Approved for public release; distribution unlimited.		
17. DISTRIBUTION STATEMENT (of the abstract entered in Block 20, if different from Report)		
18. SUPPLEMENTARY NOTES		
19. KEY WORDS (Continue on reverse side if necessary and identify by block number) Magnetohydrodynamics Sausage Instability Boundary-Integral Method Z-Pinch Rayleigh-Taylor Instability Flute Instability		
20. ABSTRACT (Continue on reverse side if necessary and identify by block number) Rayleigh-Taylor fluid instabilities are studied in the ideal magnetohydrodynamic (MHD) limit by applying boundary integral mathematical formulations to solve Laplace's equation with Dirichlet conditions on complicated boundaries. Instabilities in both the flute and sausage modes are studied for an accelerating thin cylindrical plasma, and calculations demonstrate the basic nonlinear dynamics of the z-pinch geometry. The dynamics and mathematics of plane thin shells and thin shells in cylindrical geometries with axisymmetric flow are discussed.		

DD FORM 1 JAN 73 1473 EDITION OF 1 NOV 65 IS OBSOLETE

UNCLASSIFIED

SECURITY CLASSIFICATION OF THIS PAGE (When Data Entered)

I. INTRODUCTION

In general, when a material layer is accelerated by a light pusher such as provided by magnetic pressure, the flow is unstable to the Rayleigh-Taylor instability at the interfaces. A perturbed uniform layer rapidly forms a spike-bubble structure and may even rupture. It has been shown previously (Verdon et al. 1982) that the basic dynamics of this instability process in real, incompressible fluids can be understood on the basis of the irrotational flow of layers of ideal, incompressible fluids.

In the present work for the AFWL, we have studied the instability of fluid layers driven by $\vec{J} \times \vec{B}$ forces. In the ideal magnetohydrodynamic (MHD) limit the current distribution of a SHIVA device lies on the surface of the accelerating foil so that the $\vec{J} \times \vec{B}$ force acts as a pressure normal to the surface of the foil. The methods and calculations reported here demonstrate the basic nonlinear dynamics of the accelerating foil. Instabilities of both flute and sausage character are studied.

In Section II, we review the mathematical formulation of the motion of accelerating ideal fluid layers.

Distribution For	
DDI / DAAI	<input checked="" type="checkbox"/>
DDI	<input type="checkbox"/>
DDI / DAAI	<input type="checkbox"/>
Distribution	
Distribution/	
Availability Codes	
Avail and/or	
Special	

A

In Section III, we demonstrate the equivalence of a time-dependent pressure drive and a gravity drive for planar geometries. We also discuss the dynamics of plane thin shells and thin shells in cylindrical geometries. In Section IV, the mathematics of axisymmetric flow are discussed.

II. MATHEMATICAL FORMULATION

The irrotational flow of an incompressible, inviscid fluid with constant density is completely specified by knowledge of the velocity potential ϕ which must satisfy Laplace's equation wherever the fluid lies. In order to determine ϕ , conditions must be given at the surfaces of the fluid. Bernoulli's equation may be used as an evolution equation to specify ϕ at the surfaces. Thus the mathematical problem is to solve Laplace's equation with Dirichlet conditions on complicated boundaries. There are several boundary integral formulations that solve such problems; in particular, source or dipole distributions may be used which lead to Fredholm integral equations of the first or second kind respectively. The mathematical properties of Fredholm integral equations of the second kind guarantee efficient numerical techniques for their solution, thus providing a decided advantage to the use of dipole distributions. Of course, one cannot solve all potential problems via dipole distributions alone; there are occasions where contributions from a source or sink must be included, but this step is relatively straightforward.

Suppose that an incompressible, inviscid fluid of density ρ lies between two surfaces \vec{x}_1 and \vec{x}_2 .

Adjacent to the fluid layer, there lies fluid so low in density that the region it occupies may be considered effectively a vacuum, yet it is capable of supporting an external pressure. Alternatively the region is a vacuum but there are external surface forces present such as a $\vec{J} \times \vec{B}$ force where \vec{J} is restricted to lie in the surface. In either case, assume that the external pressure is constant, but with different values p_1 and p_2 in each external region adjacent to \vec{x}_1 and \vec{x}_2 , respectively; see Figure 1 for a schematic of the flow geometry. Clearly the pressure difference will accelerate the fluid layer, inducing a mean flow.

Thus the velocity potential may be written as

$$\phi = \phi_D + \phi_E \quad (1)$$

where ϕ_E accounts for the mean (external) flow and ϕ_D may be expressed in terms of dipole distributions along each surface s_i

$$\phi_D(p) = \sum_{i=1}^2 \int_{s_i} \mu_i(q) \hat{n}(q) \cdot \nabla_q G(p,q) dq \quad (2)$$

where p, q are field points, G is the free space Green's function, \hat{n} is the normal as shown in Figure 1, and ∇_q is the gradient operator with respect to q . The choice for ϕ_E depends on the geometrical

configuration of the layer; specific cases will be discussed later.

The velocity \vec{u} of the surfaces may be calculated from $\vec{u} = \nabla \phi$. In particular, the velocity potential ϕ_D takes on the values ϕ_{Di} at the surfaces s_i respectively, where

$$\begin{aligned} \phi_{D1}(p) = & \oint_{s_1} \mu_1(q) \hat{n}(q) \cdot \nabla_q G(p, q) dq + \int_{s_2} \mu_2(q) \hat{n}(q) \cdot \nabla_q G(p, q) dq \\ & + \frac{1}{2} \mu_1(p) (p \in s_1) \end{aligned} \quad (3)$$

$$\begin{aligned} \phi_{D2}(p) = & \int_{s_1} \mu_1(q) \hat{n}(q) \cdot \nabla_q G(p, q) dq + \oint_{s_2} \mu_2(q) \hat{n}(q) \cdot \nabla_q G(p, q) dq \\ & - \frac{1}{2} \mu_2(p) (p \in s_2) \end{aligned} \quad (4)$$

Tangential derivatives of ϕ_{Di} together with the external flow give the tangential velocities of the surface, but the normal component obtained by differentiating (2) involves an awkward integral to be performed and it is preferable to proceed via a different approach.

Introduce the vector potential \vec{A}

$$\vec{u} = \nabla \times \vec{A}, \quad \text{with} \quad \nabla \cdot \vec{A} = 0 \quad (5)$$

In terms of dipole distributions

$$A(p) = \sum_{i=1}^2 \int_{s_i} \mu_i(q) \hat{n}(q) \times \nabla_q G(p, q) dq \quad (6)$$

and the normal velocity follows from $\hat{n} \cdot (\nabla \times \vec{A})$ which involves only tangential derivatives of \vec{A} . Thus, once μ_i are known, the surface velocity \vec{u}_i may be computed as described above and the surface locations updated in time.

So far the kinematics have been satisfied; the dynamic considerations provide an evolution equation for μ_i . The starting point is Bernoulli's equation evaluated at the surfaces,

$$\rho \frac{\partial \phi_{Di}}{\partial t} + \rho \frac{\partial \phi_E}{\partial t} - \frac{\rho}{2} (\vec{u}_i)^2 + p_i = c(t) \quad (i=1,2) \quad (7)$$

The partial time derivative is Lagrangian in that it represents the change in the velocity potential following the surface motion. The substitution of (3) and (4) into (7) leads directly to Fredholm integral equations of the second kind for $\frac{\partial \mu_i}{\partial t}$ of the form;

$$\begin{aligned} & \frac{\partial \mu_1}{\partial t}(p) + 2 \int_{s_1} \frac{\partial \mu_1}{\partial t}(q) \hat{n}(q) \cdot \nabla_q G(p, q) dq \\ & + 2 \int_{s_2} \frac{\partial \mu_2}{\partial t}(q) \hat{n}(q) \cdot \nabla_q G(p, q) dq = R_1(\mu_1, \mu_2, p_1, \phi_E) \quad (p \in s_1), \end{aligned} \quad (8)$$

$$\begin{aligned} & \frac{\partial \mu_2}{\partial t}(p) + 2 \int_{s_1} \frac{\partial \mu_1}{\partial t}(q) \hat{n}(q) \cdot \nabla_q G(p, q) dq \\ & + 2 \int_{s_2} \frac{\partial \mu_2}{\partial t}(q) \hat{n}(q) \cdot \nabla_q G(p, q) dq = R_2(\mu_1, \mu_2, p_2, \phi_E)(p \in s_2) \quad (9) \end{aligned}$$

where R_i contains all terms without $\frac{\partial \mu_i}{\partial t}$.

The homogeneous parts of equations (8) and (9) have nontrivial solutions which reflect the fact the velocity potential is determined only up to a constant. According to the Fredholm alternative, equations (8) and (9) have solutions only if R_i obey a certain condition. Let τ_i be the solutions to the adjoint equations,

$$\begin{aligned} & \tau_1(p) - 2 \int_{s_1} \tau_1(q) \hat{n}(p) \cdot \nabla_p G(p, q) dq \\ & - 2 \int_{s_2} \tau_2(q) \hat{n}(p) \cdot \nabla_p G(p, q) dq = 0, \quad (p \in s_1) \quad (10) \end{aligned}$$

$$\begin{aligned} & \tau_2(p) + 2 \int_{s_1} \tau_1(q) \hat{n}(p) \cdot \nabla_p G(p, q) dq \\ & + 2 \int_{s_2} \tau_2(q) \hat{n}(p) \cdot \nabla G(p, q) dq = 0, \quad (p \in s_2) \quad (11) \end{aligned}$$

then the condition for a solution to (8) and (9) is

$$\int_{s_1} R_1 \tau_1 dp + \int_{s_2} R_2 \tau_2 dp = 0 \quad (12)$$

This condition actually provides a relationship between p_1 , p_2 and the external flow ϕ_E . In the following sections, we will consider various geometrical configurations of accelerating thin fluid layers, in which case the form of ϕ_E will be known since it must describe the potential flow that accelerates the fluid layers. The strength of the acceleration may be directly related to the pressure difference $p_1 - p_2$ across the fluid layer by means of (12).

III. PLANAR LAYERS AND CYLINDRICAL FLUTE MODES

For planar, two-dimensional fluid flow (see Figure 1a) the external velocity potential is obviously

$$\phi_E = iv(t)y \quad (13)$$

where $v(t)$ is the external, uniform velocity of the fluid layer. It is convenient to introduce complex notation and to let $z = x + iy$ describe a field point. The surface locations may then be parametrized as $z_j(\alpha) = x_j(\alpha) + iy_j(\alpha)$, $j = 1, 2$. The vector potential, which has only one component the streamfunction ψ , may be combined with the velocity potential ϕ into the complex potential $\Phi = \phi + i\psi$. In particular

$$\Phi_E = -iv(t)z \quad (14)$$

The motion of the fluid surfaces is described by

$$\frac{\partial z_j^*}{\partial t} = q_j^* = \frac{\partial \Phi}{\partial \alpha} \bigg/ \frac{\partial z_j}{\partial \alpha} - iv(t) \quad (15)$$

where the star superscript implies complex conjugation. The derivation of (15) and subsequent equations follow closely the approach adopted in Baker et al (1982). The

Fredholm integral equations for $\frac{\partial \mu_j}{\partial t}$ are

$$\begin{aligned} \frac{\partial \mu_1}{\partial t}(\alpha) - \operatorname{Re} \left\{ \frac{1}{\pi i} \oint \frac{\partial \mu_1}{\partial t}(\alpha') \frac{z_{1\alpha}(\alpha') d\alpha'}{z_1(\alpha) - z_1(\alpha')} \right. \\ \left. + \frac{1}{\pi i} \int \frac{\partial \mu_2(\alpha')}{\partial t} \frac{z_{2\alpha}(\alpha') d\alpha'}{z_1(\alpha) - z_2(\alpha')} \right\} = q_1 + 2 \frac{dv}{dt} y_1 \quad (16) \end{aligned}$$

$$\begin{aligned} \frac{\partial \mu_2}{\partial t}(\alpha) + \operatorname{Re} \left\{ \frac{1}{\pi i} \int \frac{\partial \mu_1}{\partial t}(\alpha') \frac{z_{1\alpha}(\alpha') d\alpha'}{z_2(\alpha) - z_1(\alpha')} \right. \\ \left. + \frac{1}{\pi i} \oint \frac{\partial \mu_2}{\partial t}(\alpha') \frac{z_{2\alpha}(\alpha') d\alpha'}{z_2(\alpha) - z_2(\alpha')} \right\} = q_2 - 2 \frac{dv}{dt} y_2 \quad (17) \end{aligned}$$

where the subscript α implies differentiation with respect to α and

$$\begin{aligned} q_1 = \operatorname{Re} \left\{ \frac{1}{\pi i} \oint \frac{\mu_1(\alpha')}{z_1(\alpha) - z_1(\alpha')} \left[q_{1\alpha}(\alpha') - \frac{q_1(\alpha) - q_1(\alpha')}{z_1(\alpha) - z_1(\alpha')} z_{1\alpha}(\alpha') \right] d\alpha' \right. \\ \left. + \frac{1}{\pi i} \int \frac{\mu_2(\alpha')}{z_1(\alpha) - z_2(\alpha')} \left[q_{2\alpha}(\alpha') - \frac{q_1(\alpha) - q_2(\alpha')}{z_1(\alpha) - z_2(\alpha')} z_{2\alpha}(\alpha') \right] d\alpha' \right\} \\ - q_1 q_1^* + 2p_1 \quad (18) \end{aligned}$$

$$\begin{aligned}
q_2 = & -\text{Re} \left\{ \frac{1}{\pi i} \int \frac{\mu_1(\alpha')}{z_2(\alpha) - z_1(\alpha')} \left[q_{1\alpha}(\alpha') - \frac{q_2(\alpha) - q_1(\alpha')}{z_2(\alpha) - z_1(\alpha')} z_{1\alpha}(\alpha') \right] d\alpha' \right. \\
& + \frac{1}{\pi i} \int \frac{\mu_2(\alpha')}{z_2(\alpha) - z_2(\alpha')} \left[q_{2\alpha}(\alpha') - \frac{q_2(\alpha) - q_2(\alpha')}{z_2(\alpha) - z_2(\alpha')} z_{2\alpha}(\alpha') \right] d\alpha' \left. \right\} \\
& + q_2 q_2^* - 2p_2
\end{aligned} \tag{19}$$

In order for (17) and (18) to have a solution, the condition (12) must be satisfied; thus

$$2 \frac{dv}{dt} \left[\int y_2 \tau_2 d\alpha + \int y_1 \tau_1 d\alpha \right] = \int q_2 \tau_2 d\alpha - \int q_1 \tau_1 d\alpha \tag{20}$$

For given p_1 and p_2 , (20) determines $\frac{dv}{dt}$. The form of the equations (16) and (17) is identical to those for a fluid layer falling under the influence of gravity with $g = -\frac{dv}{dt}$.

The above analysis demonstrates the equivalence of pressure drive (normal to the surface) in planar geometries and a time-dependent gravity drive (in a fixed direction). Eq. (20) guarantees conservation of momentum in these systems and so determines the mean acceleration of the layer.

The numerical solution to (15), (16), and (17) follows a standard approach adopted by Baker et al (1982). We present here the results for $\frac{dv}{dt} = -1$. The initial profile has the form

$$z_1 = \alpha + i$$

$$z_2 = \alpha + i 0.06 \pi \cos \alpha.$$

Figure 2 shows the evolution in time of the surface locations. A clearly observed spike develops and the layer thickness of the bubble thins dramatically. Figure 3 shows the layer thickness at the bubble center as a function of time. Unfortunately, the code presently is not accurate beyond a time of approximately 4. Further calculations in time require a modification of the numerical quadrature for the integrals in (16), (17), (18), and (19).

Next, we consider cylindrical geometry as shown in Figure 1b. The external velocity potential now has the form

$$\phi_E = - A(t) \log(z) \quad (21)$$

An equation similar to (20) is easily obtained, but there is an important difference between the previous case and the present one; the external flow no longer has the appearance of that induced by a gravity field. Numerical calculations give the results shown in Figure 4. The spike and bubble structure are different from those observed in Figure 2.

Finally, in the next section, we present the mathematical formulation for axisymmetric flow, which is somewhat different from that considered in this section.

IV. AXISYMMETRIC FLOW AND SAUSAGE MODES

The generalized vortex method of Baker, Meiron and Orszag (1980,1982) is a boundary integral technique applied to free surface flow in incompressible, inviscid fluid which contain regions of constant, but different densities. When the free surface lies between fluid and vacuum, a simpler, but equivalent method may be used. This method is described in some generality before being applied to axisymmetric flow.

The free surface is represented as a dipole layer of strength μ . The velocity potential ϕ may then be written as

$$\phi(p) = \int \mu(q) \frac{\partial G}{\partial n}(p,q) dq \quad (22)$$

where G is the free space Green's function for Laplace's equation, p and q are field points and n is an outward normal. For convenience we assume that the free surface is smooth (has a continuous normal) and closed; an open surface may be considered as a particular limit of a closed surface. The normal derivative of G is

taken with respect to q , keeping p fixed. As p approaches the free surface along the normal, the potential takes on different values on either side

$$\phi_I(p) = \oint \mu(q) \frac{\partial G}{\partial n}(p, q) dq + \frac{\mu}{2}(p) \quad (23)$$

as p tends to the surface from the inside and

$$\phi_O(p) = \oint \mu(q) \frac{\partial G}{\partial n}(p, q) dq - \frac{\mu}{2}(p) \quad (24)$$

as p tends to the surface from the outside. Clearly,

$$\mu(p) = \phi_I(p) - \phi_O(p).$$

If $\mu(p)$ is known, then the potential can be evaluated from (22) and the fluid velocity follows from $\vec{u} = \nabla \phi$. Alternatively one may obtain the fluid velocity from the velocity vector potential \vec{A} ; $\vec{u} = \nabla \times \vec{A}$. For a dipole layer

$$\vec{A}(p) = \oint \mu(q) \hat{n} \times \nabla G(p, q) dq \quad (25)$$

where the gradient is taken with respect to q and \hat{n} is the unit outward normal. As p tends to the surface, $\vec{A}(p)$ is continuous.

Normally in free surface flow problems, the velocity is required only at the surface in order to update its location. This is easily accomplished if μ is known.

In fact, the tangential velocity components can be computed from $\nabla\phi$ and the normal component from $\nabla \times \vec{A}$. In both cases, only tangential derivatives are required thus avoiding the more complicated and more difficult evaluation of normal derivatives.

The basis of the generalized vortex method is the use of an evolution equation for μ derived from Bernoulli's equation, by which μ is updated and the free surface velocity calculated as described above. The method involves evaluating the time derivatives of (23), (24) and (25), which, in the case of axisymmetric flow, is tedious algebraically and presents difficulties numerically. However, if one is interested in the flow of a free surface between fluid and vacuum one may use Bernoulli's equation directly to update the potential at the free surface as it moves. Then (23) or (24) is used as a Fredholm integral equation of the second kind for μ . Finally, knowing μ, \vec{A} is computed from (25) and the free surface velocity is computed as described above. This is the approach adopted for axisymmetric free surface flow.

Introduce a cylindrical coordinate system (R, θ, z) where R is the radius, θ the azimuthal angle and z the axial position. The free surface is parametrized by $R(e, t)$ and $z(e, t)$. Let $I(e)$ be the principal-value integral in (23) and (24)

$$I(e) = \frac{1}{2\pi} \oint \frac{\mu(e') de'}{[(z(e)-z(e'))^2 + (R(e)+R(e'))^2]^{1/2}} \left\{ z_e(e') K(k) \right. \\ - \frac{z_e(e') [(z(e)-z(e'))^2 + R^2(e) - R^2(e')] - 2R(e') R_e(e') (z(e)-z(e'))}{(z(e)-z(e'))^2 + (R(e)-R(e'))^2} \\ \left. \times E(k) \right\} \quad (26)$$

where $K(k)$ and $E(k)$ are the complete elliptic integrals of the first and second kinds respectively, the subscript e refers to differentiation with respect to e (t fixed) and

$$k^2 = \frac{4R(e)R(e')}{(z(e)-z(e'))^2 + (R(e)+R(e'))^2} \quad (27)$$

The only non-vanishing component of $\vec{\Lambda}$ is the azimuthal component, expressed as ψ/R , where ψ plays the role of the streamfunction in axisymmetric flow. At the surface,

$$\psi(e) = \frac{1}{2\pi} \oint \frac{\mu(e') de'}{[(z(e)-z(e'))^2 + (R(e)+R(e'))^2]^{1/2}} \\ \left\{ [z_e(e') (z(e)-z(e')) - R(e') R_e(e')] K(k) \right. \\ - [z_e(e') (z(e)-z(e')) - R(e') R_e(e')] \\ \times \frac{(z(e)-z(e'))^2 + R^2(e) + R^2(e') + 2R^2(e) R(e') R_e(e')}{(z(e)-z(e'))^2 + (R(e)-R(e'))^2} E(k) \left. \right\} \quad (28)$$

The radial and axial velocity components, u and w respectively, are given by

$$u = \frac{\partial \phi}{\partial R} = \frac{1}{R} \frac{\partial \psi}{\partial z} \quad (29a)$$

$$w = \frac{\partial \phi}{\partial z} = - \frac{1}{R} \frac{\partial \psi}{\partial R} \quad (29b)$$

To update the free surface, the velocity components at the surface must be known. They can be expressed in terms of the derivatives of ϕ and ψ along the surface. Using (29) one finds

$$\phi_e = R_e \frac{\partial \phi}{\partial R} + z_e \frac{\partial \phi}{\partial z} = R_e u + z_e w \quad (30a)$$

$$\psi_e = R_e \frac{\partial \psi}{\partial R} + z_e \frac{\partial \psi}{\partial z} = R(z_e u - R_e w) \quad (30b)$$

where ϕ will either be ϕ_I or ϕ_O depending on which side of the interface the fluid lies. Inverting the above equations, one obtains

$$\frac{\partial R}{\partial t} = u = (R_e \phi_e + z_e \psi_e / R) / s_e^2 \quad (31a)$$

$$\frac{\partial z}{\partial t} = w = (z_e \phi_e - R_e \psi_e / R) / s_e^2 \quad (31b)$$

as the evolution equations for the surface's location,
where

$$s_e^2 = R_e^2 + z_e^2 \quad (32)$$

Finally, Bernoulli's equation is used as an evolution equation for ϕ . As a specific example, consider a spherical bubble that is compressed by an external pressure gradient in the fluid. Write the potential as

$$\phi = \frac{A(t)}{[R^2 + z^2]^{1/2}} + \tilde{\phi} \quad (33)$$

where A is the strength at a sink (or source, if $A < 0$) placed at center of the bubble. After substituting (33) into Bernoulli's equation, one finds at the surface

$$\frac{\partial \tilde{\phi}}{\partial t} - \frac{1}{2} \left[\left(\frac{\partial \tilde{\phi}}{\partial R} \right)^2 + \left(\frac{\partial \tilde{\phi}}{\partial z} \right)^2 \right] + \frac{\frac{dA}{dt}}{[R^2 + z^2]^{1/2}} + \frac{1}{2} \frac{A^2}{[R^2 + z^2]^2} + P_I = P_O \quad (34)$$

where the time derivative is taken following the motion described by (31) the fluid is assumed stationary far from the bubble with pressure P_O , the density is 1 and P_I is the pressure inside the bubble. If the bubble is a perfect sphere, one may set $\tilde{\phi} = 0$ and $\rho^2 = R^2 + z^2$ so that (31) and (34) become

$$\frac{1}{\rho} \frac{dA}{dt} + \frac{A^2}{2\rho^4} = P_0 - P_I \quad (35)$$

$$\frac{d\rho}{dt} = - \frac{A}{\rho^2} \quad (36)$$

We may subtract (35) from (34) to obtain

$$\frac{\partial \tilde{\phi}}{\partial t} - \frac{1}{2}(\tilde{u}^2 + \tilde{w}^2) + \frac{dA}{dt} \left[\frac{1}{[R^2 + z^2]^{1/2}} - \frac{1}{\rho} \right] + \frac{A^2}{2} \left[\frac{1}{(R^2 + z^2)^2} - \frac{1}{\rho^4} \right] = 0 \quad (37)$$

Also,

$$\frac{\partial R}{\partial t} = \tilde{u} - \frac{AR}{[R^2 + z^2]^{3/2}} \quad (38a)$$

$$\frac{\partial z}{\partial t} = \tilde{w} - \frac{Az}{[R^2 + z^2]^{3/2}} \quad (38b)$$

where \tilde{u} and \tilde{w} are computed from the dipole representation for $\tilde{\phi}$ as described. The above equations, (35), (36), (37) and (38) constitute a set of evolution equations for the motion of the bubble surface.

The method of solution is as follows. Suppose A , ρ , R , z and $\tilde{\phi}$ are all known at some given time. The time derivatives of A and ρ are known from (35) and (36). We then solve for μ by iteration from (24) with $\phi_0 = \tilde{\phi}$.

$$\mu_{n+1}(e) = -2\tilde{\phi}(e) + 2I_n(e) \quad (39)$$

where $I_n(e)$ represents $I(e)$ with $\mu(e')$ replaced by $\mu_n(e')$. The iteration process is known to be globally convergent. Moreover standard extrapolation techniques may be used to ensure that only a few (2 - 3) iterations are required for accurate results. Knowing $\mu(e)$, $\psi(e)$ is computed from (28) and then \tilde{u} and \tilde{w} are determined from (31). Finally, the time derivatives of ϕ , R and z are evaluated by (37) and (38) and the surface may be updated.

To execute this method of solution numerically requires some care. Points evenly distributed in e are introduced as a discrete representation for the surface. All derivatives in e are approximated by spline derivatives. The difficulties lie in the numerical evaluation of the integrals (26) and (28). The complete elliptic integral of the first kind, $K(k)$, has a logarithmic singularity as $k \rightarrow 1$ which occurs when $e' \rightarrow e$. The complete elliptic integral of the second kind behaves as

$$(e'-e)\log|e'-e|$$

as $e' \rightarrow e$. A further complication is the fact that, for e close to the axis, k varies from 0 at the axis to 1 at $e' = e$. This rapid variation in k must be accounted for in any accurate numerical quadrature.

The integrals may be regularized by using the fact that, when $\mu = 1$, $I(e) = \frac{1}{2}$ and $\psi(e) = 0$. In addition,

a particular quadrature has been devised to account for the presence of terms containing logarithms. Suppose that the parametrization of the free surface is such that $0 \leq e \leq \pi$ and $R(0) = R(\pi) = 0$, that is $e = 0, \pi$ correspond to the poles of the bubble. $K(k)$ and $E(k)$ may be approximated by

$$K(k) = A_K(m) - B_K(m) \log |m| \quad (40a)$$

$$E(k) = A_E(m) - B_E(m) \log |m| \quad (40b)$$

where $m = 1 - k^2$ and $A_K(m)$, $A_E(m)$, $B_K(m)$ and $B_E(m)$ are polynomials in m (see Abramowitz and Stegun, 1964). Thus one may split the integrals into parts that contain logarithms or not. Define

$$F(A,B) = \frac{\mu(e') - \mu(e)}{[(z(e) - z(e'))^2 + (R(e) + R(e'))^2]^{1/2}} \left\{ z_e(e') A - \frac{z_e(e') [(z(e) - z(e'))^2 + R^2(e) - R^2(e')] - 2R(e') R_e(e') (z(e) - z(e'))}{(z(e) - z(e'))^2 + (R(e) - R(e'))^2} B \right\} \quad (41)$$

$$I_1 = \frac{\mu(e)}{2} + \frac{1}{2\pi} \int_0^\pi F(A_K, A_E) de' \quad (42)$$

$$I_2 = \frac{1}{2\pi} \int_0^\pi F(B_K, B_E) [\log |m| - \log |q|] de' \quad (43)$$

$$I_3 = \frac{1}{2\pi} \int_0^\pi F(B_K, B_E) \log |q| de' \quad (44)$$

Then $I = I_1 - I_2 - I_3$. Here q models the behaviour of m ; $m = 1$ at $e' = 0, \pi$ and $m = 0$ at $e' = e$, so the variation in m is rapid when e is near 0 or π . A good choice for q is

$$q = \frac{\sigma(e'-e)^2}{e'(\pi-e') + \sigma(e'-e)^2} \quad (45)$$

where $\sigma = 1/\pi^2 + \pi^2/[4e(\pi-e)]$. Since $F(A_K, A_E)$ and $F(B_K, B_E)$ are analytic, I_1 and I_2 may be evaluated by the trapezoidal rule with $O(h^2)$ accuracy, where h is the spacing in e of the points. For I_3 , a special quadrature is used. $F(B_K, B_E)$ is approximated as a piecewise continuous linear function and I_3 is then integrated analytically; this leads to

$$I_3 = \sum_j \omega_j F_j \quad (46)$$

where F_j is the value of $F(B_K, B_E)$ at e'_j . After some algebra, one finds

$$\omega_j = \frac{1}{h} \left[2A_j - A_{j+1} - A_{j-1} + (e - e'_j) (2B_j - B_{j-1} - B_{j+1}) + h(B_{j+1} - B_{j-1}) \right] \quad (47)$$

where

$$\begin{aligned} A_j &= \frac{1}{2}(e'_j - e)^2 \log \{ \sigma (e'_j - e)^2 \} \\ &- \frac{2(\sigma - 1)^2 (e'_j - e)^2 - r^2 + 2s(\sigma - 1)}{4(\sigma - 1)^2} \log \{ (\sigma - 1) (e'_j - e)^2 + r(e'_j - e) + s \} \\ &- \frac{r(e'_j - e)}{2(\sigma - 1)} + \frac{r}{2} \frac{[4s(\sigma - 1) - r^2]^{1/2}}{(\sigma - 1)^2} \tan^{-1} \left\{ \frac{2(\sigma - 1)(e'_j - e) + r}{[4s(\sigma - 1) - r^2]^{1/2}} \right\} \end{aligned} \quad (48)$$

$$\begin{aligned} B_j &= (e'_j - e) \log \{ \sigma (e'_j - e)^2 \} \\ &- \frac{2(\sigma - 1)(e'_j - e) + r}{2(\sigma - 1)} \log \{ (\sigma - 1) (e'_j - e)^2 + r(e'_j - e) + s \} \\ &- \frac{[4s(\sigma - 1) - r^2]^{1/2}}{(\sigma - 1)} \tan^{-1} \left\{ \frac{2(\sigma - 1)(e'_j - e) + r}{[4s(\sigma - 1) - r^2]^{1/2}} \right\} \end{aligned} \quad (49)$$

and $r = \pi - 2e$, $s = e(\pi - e)$.

The total quadrature error for I is of order $O(h^2)$ near the axis and is more accurate away from the axis. A quadrature for $\psi(e)$ is similarly constructed; define

$$G = \frac{[\mu(e') - \mu(e)]}{[(z(e) - z(e'))^2 + (R(e) + R(e'))^2]^{1/2}}$$

$$[z_e(e')(z(e) - z(e')) - R(e')R_e(e')] \quad (50)$$

$$H = \frac{[\mu(e') - \mu(e)]}{[(z(e) - z(e'))^2 + (R(e) + R(e'))^2]^{1/2}}$$

$$\{[z_e(e')(z(e) - z(e')) - R(e')R_e(e')]$$

$$\times [(z(e) - z(e'))^2 + R^2(e) + R^2(e')] + 2R^2(e)R(e')R_e(e')\} \quad (51)$$

$$\psi_1 = \frac{1}{2\pi} \int_0^\pi GA_K(m) \quad (52)$$

$$- H \left[\frac{1}{(z(e) - z(e'))^2 + (R(e) - R(e'))^2} - \frac{1}{s_e^2(e - e')^2} \right] A_E(m) \} de'$$

$$\psi_2 = \frac{1}{2\pi} \int_0^\pi \frac{H}{s_e^2(e' - e)} \cdot \frac{A_E(m)}{(e' - e)} de' \quad (53)$$

$$\psi_3 = \frac{1}{2\pi} \int_0^\pi [GB_K(m) \quad (54)$$

$$- \frac{H B_E(m)}{(z(e) - z(e'))^2 + (R(e) - R(e'))^2} \{ \log |m| - \log |q| \} \} de'$$

$$\psi_4 = \frac{1}{2\pi} \int_0^\pi \frac{H B_E(m)}{(z(e)-z(e'))^2 + (R(e)-R(e'))^2} \log |q| de' \quad (55)$$

Then $\psi = \psi_1 - \psi_2 - \psi_3 + \psi_4$. The integrals I_1 and I_3 are evaluated by the trapezoidal rule, and I_4 is evaluated by the special quadrature (46). However I_2 has a pole singularity, since $H \sim (e'-e)$ as e' approaches e . We devise a quadrature by approximating $\tilde{H} = HB_E(m)/[s_e^2(e'-e)]$ as a piecewise continuous linear function and integrating analytically; thus

$$\psi_2 = \sum_j \omega_j \tilde{H}_j \quad (56)$$

where

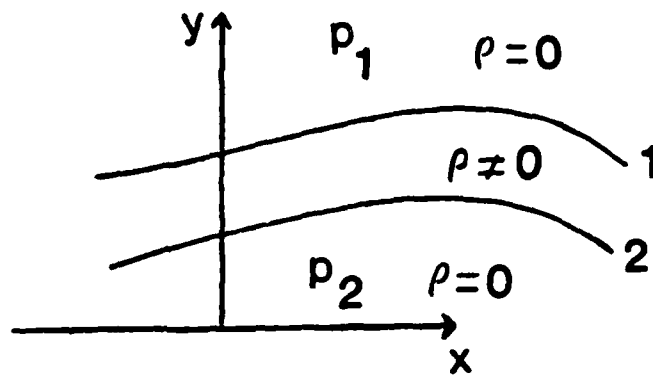
$$\begin{aligned} \omega_j = \frac{1}{h} \{ & (e'_{j+1}-e) \log |e'_{j+1}-e| \\ & + (e'_{j-1}-e) \log |e'_{j-1}-e| - 2(e'_j-e) \log |e'_j-e| \} \end{aligned} \quad (57)$$

Starting with the initial conditions $A = 0$, $\tilde{\phi} = 0$, $R = (1 + \epsilon \cos(2e)) \sin(e)$, $z = - (1 + \epsilon \cos(2e)) \cos(e)$, $\rho = 0.9703797$, the surface is discretised with 33 points and updated in time with a fourth order Adams-Bashforth method with a timestep of 0.01. The pressure difference

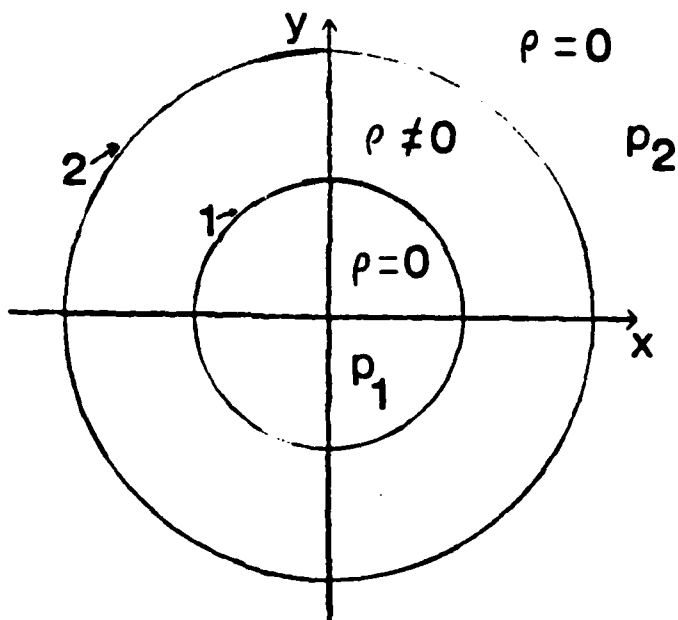
$P_0 - P_I = 1$ and $\epsilon = 0.1$. Figure 5 shows the profile of the bubble at various times. Clearly a Rayleigh-Taylor-type instability develops at the waist of the bubble and will probably lead to bubble separation into two smaller bubbles.

REFERENCES

1. Abramowitz, M., and Stegun, I.A., Handbook of Mathematical Functions, National Bureau of Standards, U.S. Government Printing Office, 1964.
2. Baker, G.R., Meiron, D.I., and Orszag, S.A., Phys. Fluids, 23, 1485-1490, 1980.
3. Baker, G.R., Meiron, D.I., and Orszag, S.A., J. Fluid Mech., 123, 477-501, 1982.
4. Verdon, C.P., McCrory, R.L., Morse, R.L., Baker, G.R., Meiron, D.I., and Orszag, S.A., Phys. Fluids, 25, 1653-1674, 1982.



(a) Flute mode.



(b) Axisymmetric sausage mode.

Figure 1. Schematic diagram of flow geometry for instability problem.

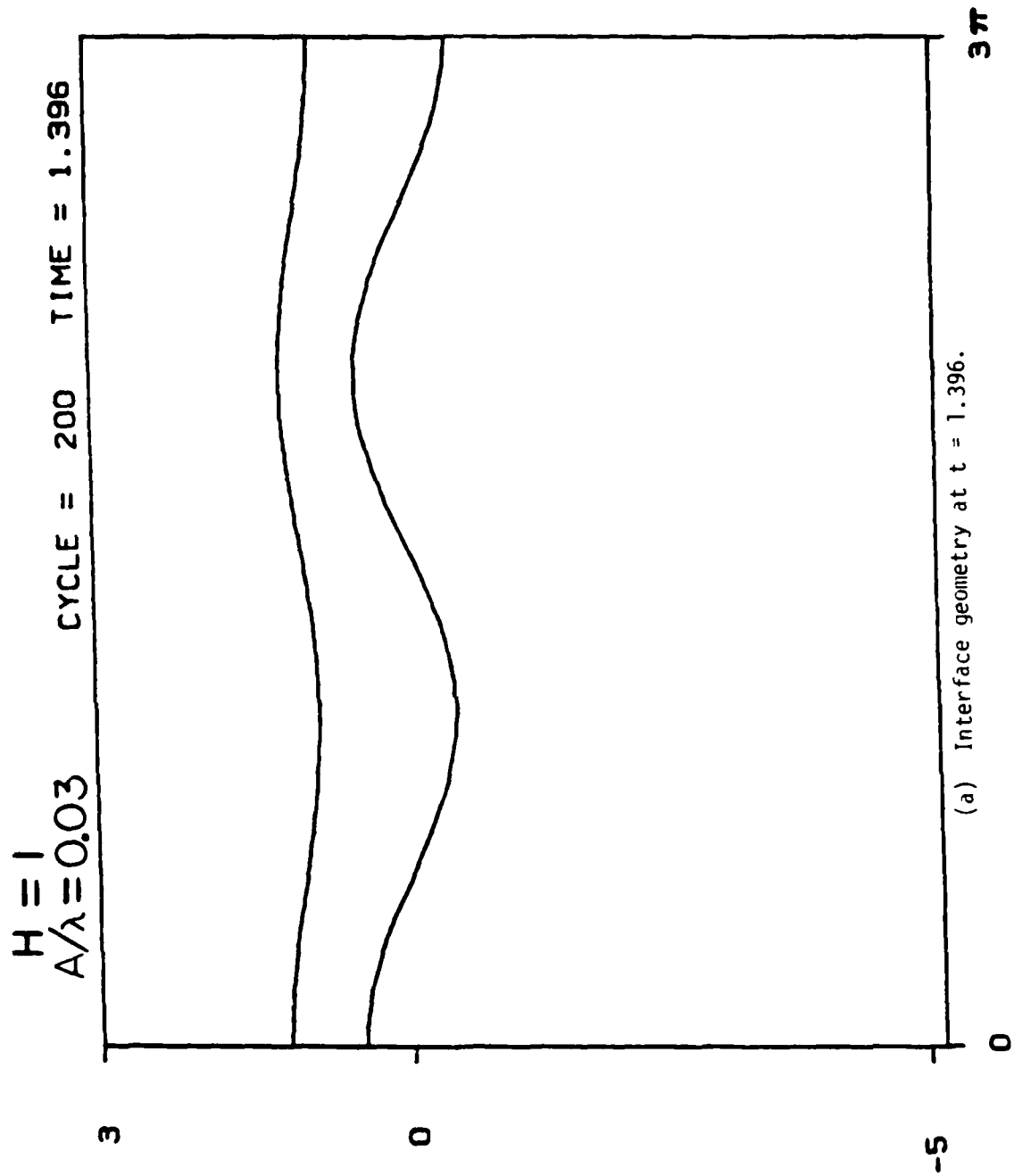
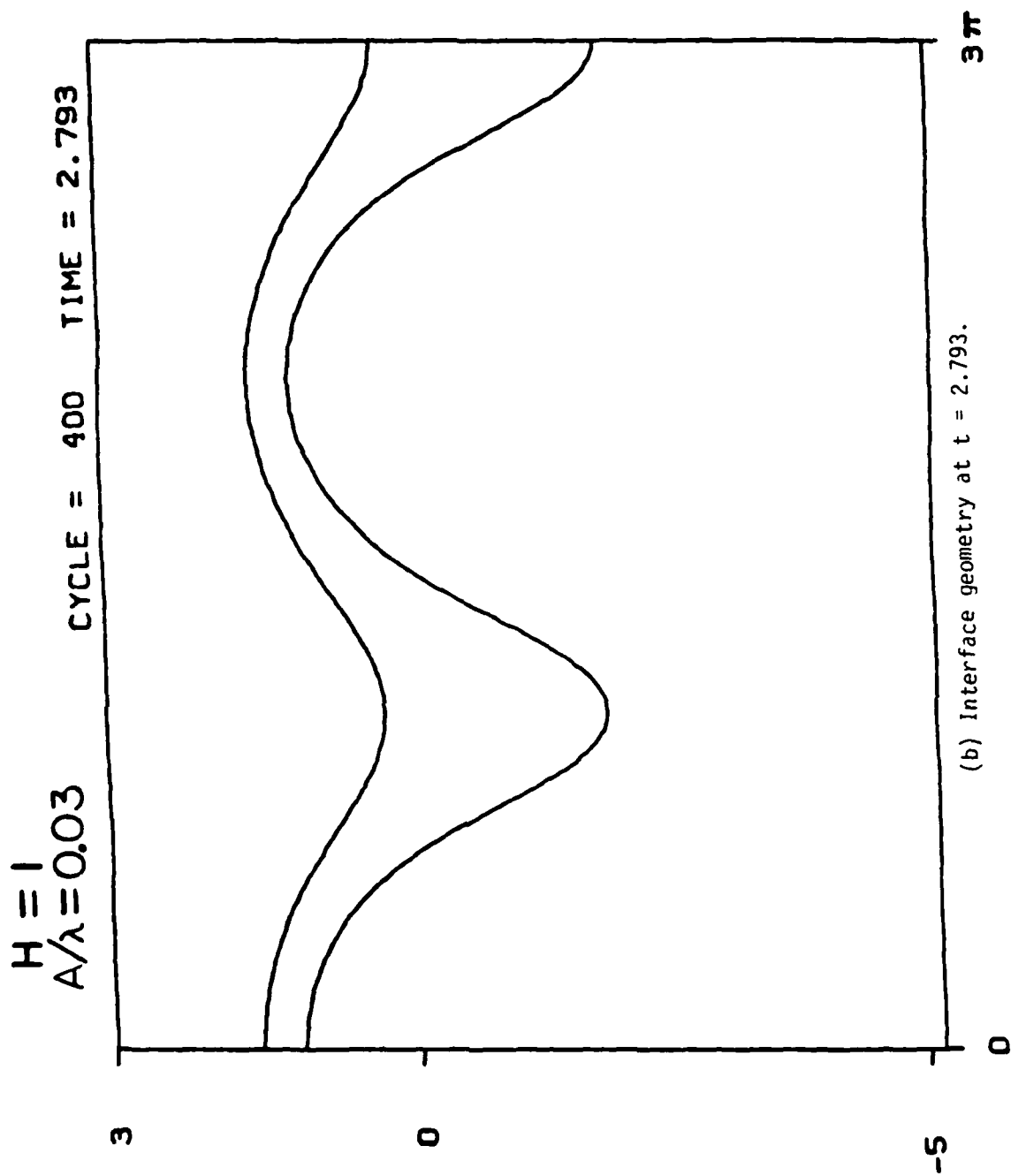


Figure 2. Results for flute mode instability problem.



(b) Interface geometry at $t = 2.793$.

Figure 2. Continued.

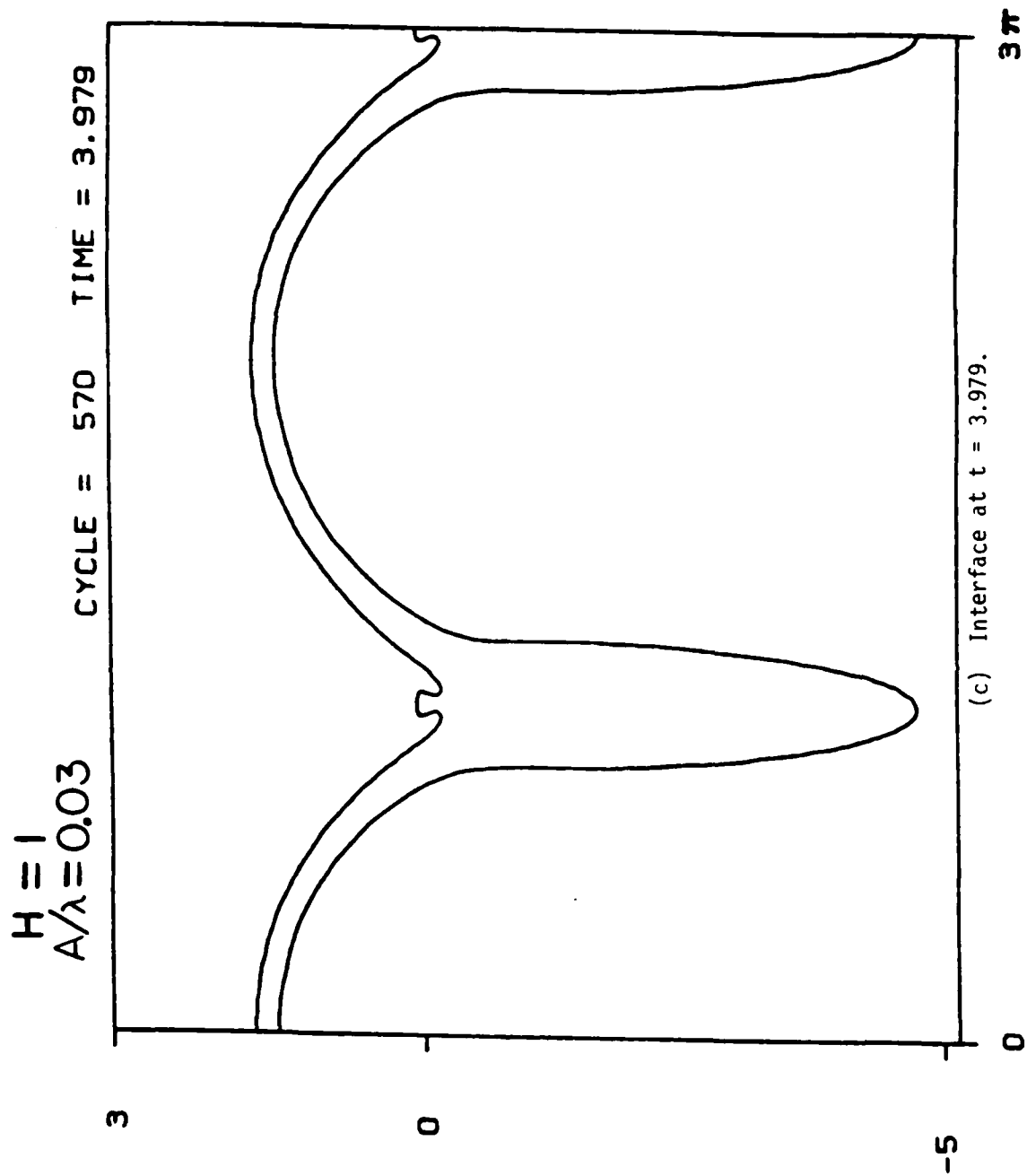


Figure 2. Concluded.

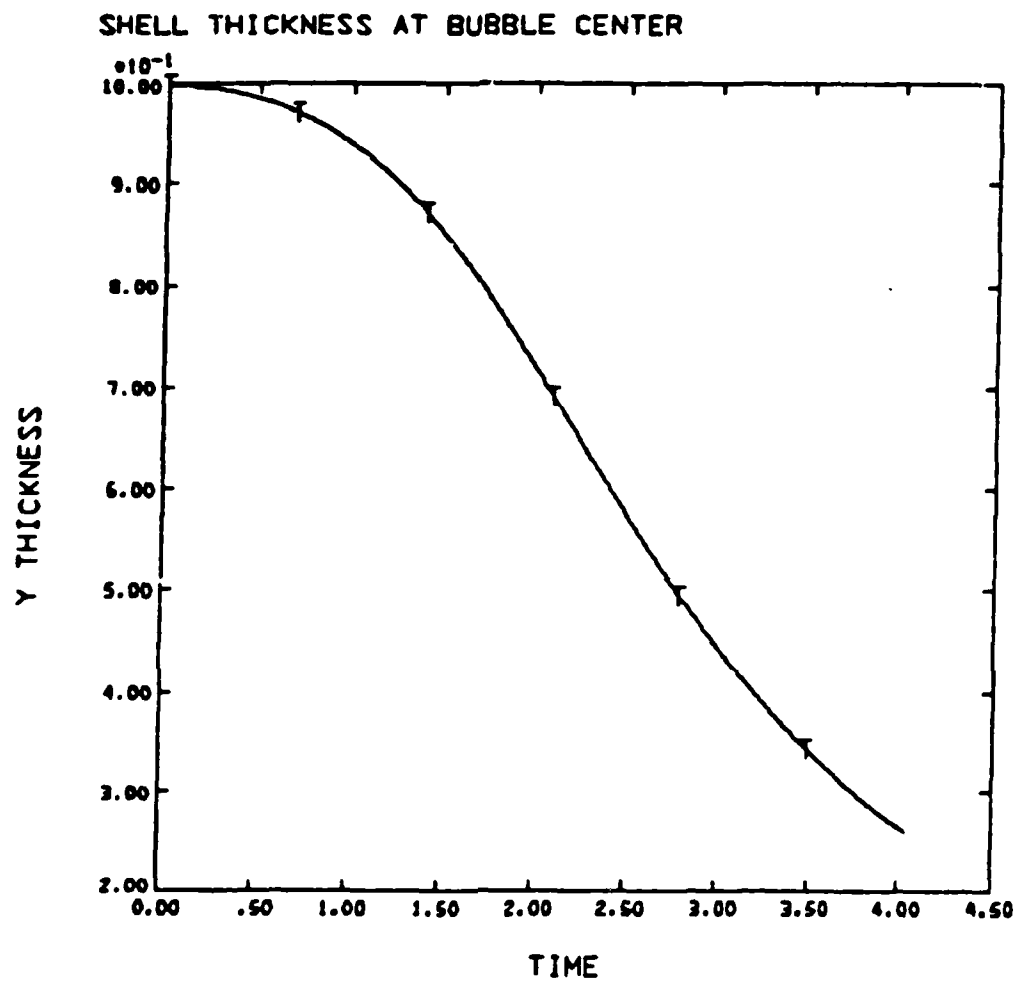
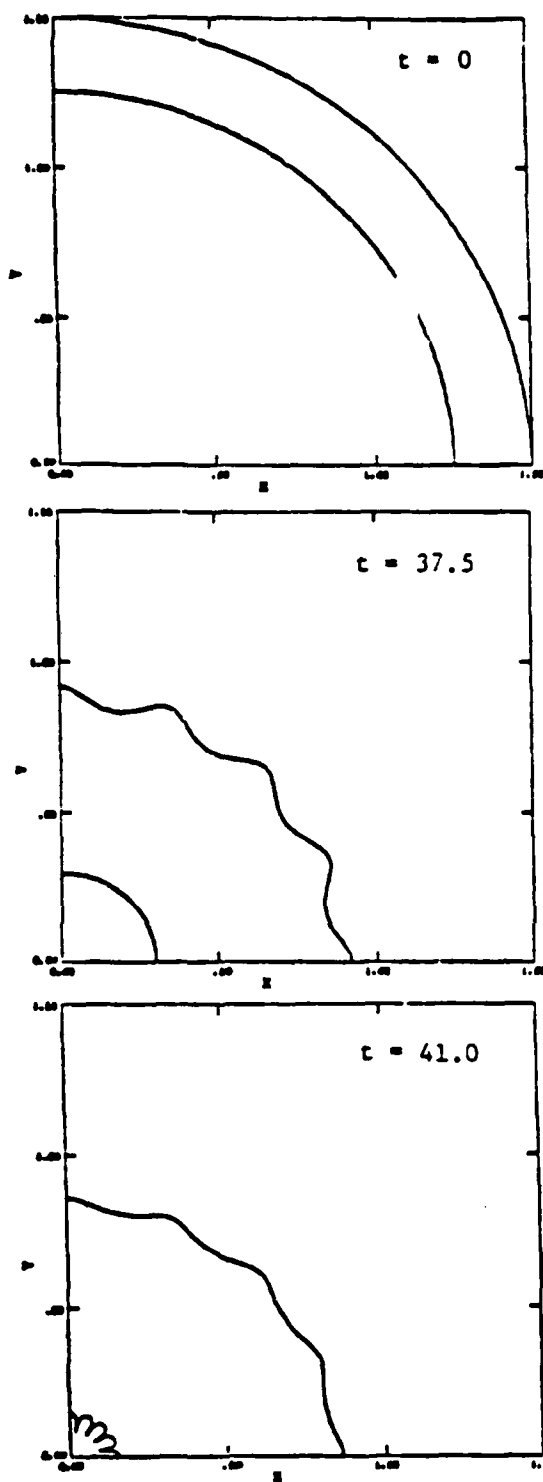
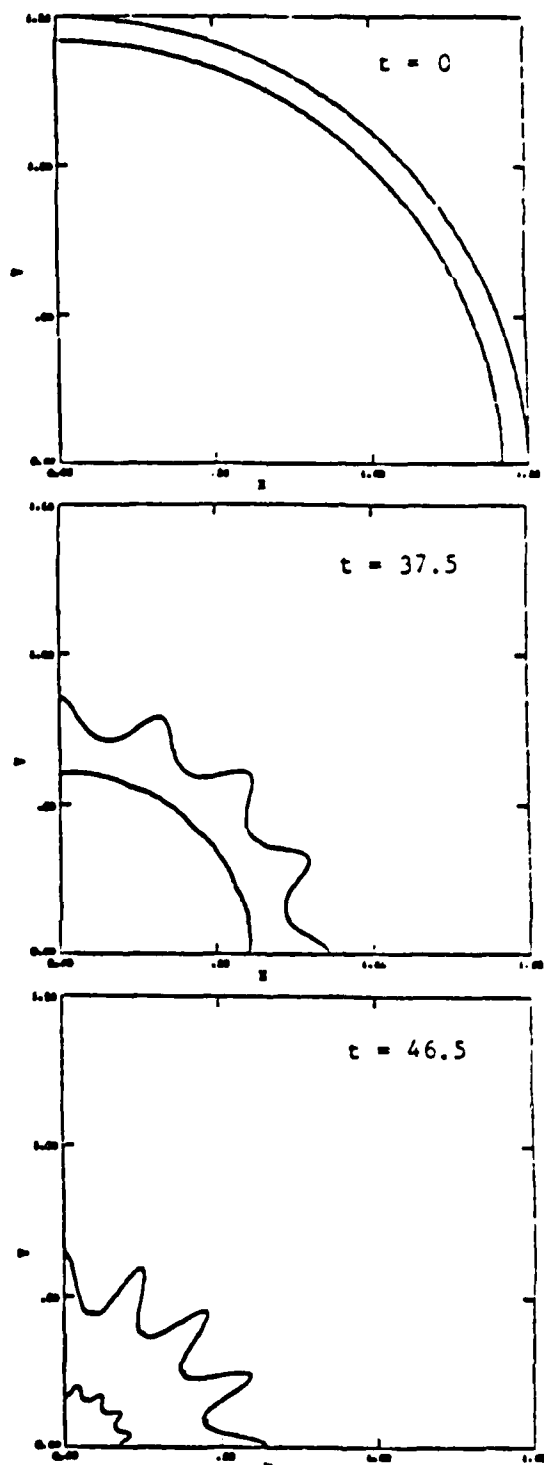


Figure 3. A plot of shell thickness versus time for the flute mode instability problem.



(a) Outside of a relatively thick shell ($k\Delta x = 3$).



(b) Outside of a shell only one-third as thick ($k\Delta x = 1$).

Figure 4. Results of a calculation with a small perturbation (0.5%).

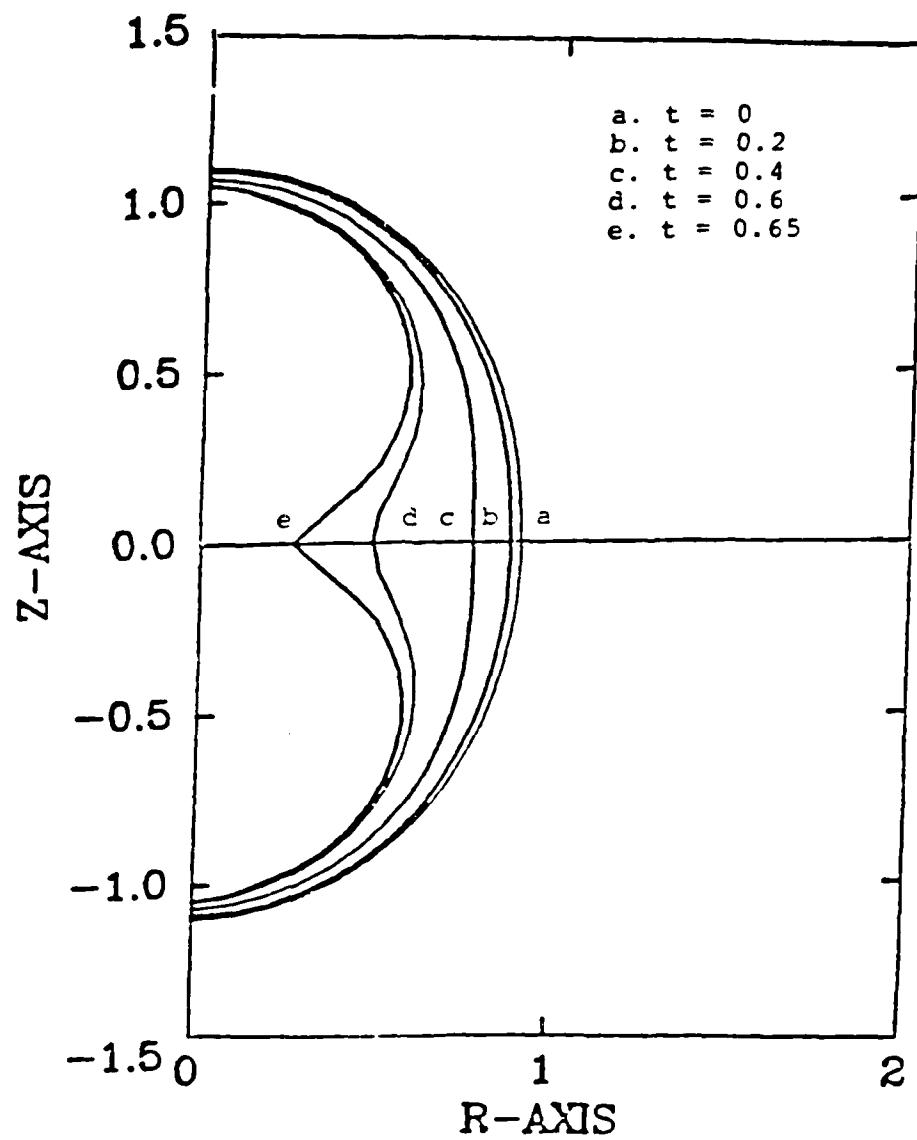


Figure 5. A plot of interface geometry versus time for the sausage mode instability problem.

